Absolute Magnitudes of Turnoff Stars in Globular Clusters Palomar 13 and Whiting 1

Kathleen Grabowski [1], Matthew Newby[1], Heidi Jo Newberg[1]

[1] Rensselaer Polytechnic Institute

May 10, 2013

We characterize the F-turnoff (FTO) stars in two globular clusters in the halo of the Milky Way. Data for the two clusters, Palomar 13 and Whiting 1, recently became available in Data Release 8 (DR8) of the Sloan Digital Sky Survey (SDSS). Based on a histogram of the magnitude distribution, we find that the mean magnitude of FTO stars in Palomar 13 is $M_g = 4.46 \pm 0.26$ and the mean magnitude of FTO stars in Whiting 1 is $M_g = 4.11 \pm 0.30$. These measurements are in good agreement with Newby et al. (2011). Palomar 13 is marginally inconsistent within $2\sigma - 3\sigma$ because fewer of the fainter stars are observed than expected. Since Palomar 13 is within the range of cluster propeties previously studied, it was not expected that this cluster would be an outlier. The discrepancy is due to lower than expected completeness in measuring faint stars in the cluster, because the seeing in the Palomar 13 images is worse than in other SDSS images of globular clusters. We continue to find that globular clusters in the halo of the Milky Way all have similar absolute magnitude distributions. We also confirm that Whiting 1 is within the Sagittarius dwarf tidal stream, while Palomar 13 is not.

1 Introduction

Stars are classified by temperature using the letters OBAFGKM listed in order from hottest to coolest. The brightness of a star is measured in magnitudes, where a decrease in magnitude of one unit(for example from 0 to -1) is an increase in brightness by a factor of 2.5. The apparent magnitude measures the brightness that a star appears to us on Earth. Absolute magnitude is a measure of how bright the star would be if it was viewed from 32.6 lightyears (10 parsecs) away. Another stellar characteristic, color, is quantified by the difference between the magnitudes in two filters. The Sloan Digital Sky Survey (SDSS)[1] measures the amount of light from each observed star through five different filters, labeled *ugriz*, representing the ultra-violet, green, red, infrared, and one micron parts of the spectrum.

In this paper we will focus specifically on stars of spectral type F. Stars with this temperature have colors of $0.1 < (g-r)_0 < 0.3$, where the zero subscript denotes that the color has been dereddened using the Schlegel, Finkbeiner, and Davis (1998) extinction map [2], to remove the effects of reddening due to dust

between us and the star.

A color-magnitude diagram, also called a Hertzsprung-Russell (HR) diagram, shows some measure of temperature on the x-axis and some measure of brightness on the y-axis. Brighter stars are towards the top of the diagram, and fainter stars are towards the bottom. See Figure 3 in Newby et al. (2011) for representative HR diagrams of globular clusters in SDSS data [3]. A globular cluster is a gravitationally bound group of hundreds of thousands of stars originally formed from one cloud of gas and dust. However, using high accuracy Hubble Space Telescope data, Piotto et al. (2012) recently showed that many globular clusters have more than one stellar population, visible from a broad subgiant branch (SBG) or distinct separation between multiple SGBs [4].

All of the stars begin on the main sequence of the HR diagram and the energy that makes them shine comes from fusion of hydrogen into helium. Although the more massive stars have more hydrogen fuel to burn, they are so much hotter and brighter than less massive stars that they run out of fuel more quickly. As these hot, bright stars move off the main sequence and eventually die, there is a most massive (most blue and bright) group of stars that is still left in the main sequence of the globular cluster. The stars in this group are known as "turnoff" stars. For most globular clusters, the color (temperature) of the stars is spectral type F (hereafter FTO stars).

Stars that have a known intrinsic brightness (absolute magnitude) are often used as distance indicators in astronomy because the intrinsic brightness can be compared with the observed brightness (apparent magnitude) to get the distance using the inverse square law. FTO stars are not traditionally chosen for distance calculations because they span a range of 1.5 magnitudes or more in brightness. When one absolute magnitude is assumed for the FTO stars in a particular globular cluster, the stars would appear to be spread in distance by a factor of 2 . However, if there are enough FTO stars in a sky survey, the statistics of the absolute magnitude distribution can be used to map the volume density of stars without knowing the distance to each individual star. This techniques is known as statistical photometric parallax (Newberg et al.(2013)) [5]. For example, Newberg et al. (2002) used F-stars to identify new halo structures [5] from spatial overdensities of SDSS stars in the Galactic halo. Even though A stars are each individually better indicators in the halo than FTO stars, the abundance of FTO stars made it possible to see many more halo substructures than Yanny et al. (2000), who used similar data and techniques but used color-selected A stars [6]. Later, Newberg and Yanny used FTO stars to estimate distances to overdensities [7] and halo streams including the Sagittarius stream [9], the Orphan stream [10], and GD-1 [11].

Some authors have measured distances and spatial stellar densities using a maximum likelihood technique [12] that assumes a Gaussian distribution in magnitude of FTO star absolute magnitudes centered at $M_g = 4.2$ in the green passband with $\sigma = 0.6$. This absolute magnitude distribution was suggested from a study

of some of the known halo substructures, but it was not known how universal the absolute magnitude distribution was. In general, the color and brightness of FTO stars depends on age and chemical composition (metallicity) of the stellar population observed. However, Newby et al. (2011) found that the absolute magnitude distribution of color-selected F stars is intrinsically similar for the eleven globular clusters in the Milky Way stellar halo that were studied. They found that the best fit to the data was a"double-sided" Gaussian distribution with a central absolute magnitude of $M_g = 4.18 \pm 0.008$ [3], a left side standard deviation of $\sigma_\ell = 0.36$, and a right side standard deviation of $\sigma_r = 0.76$. In addition, it was discovered that the observed standard deviation appears to be dependent on apparent magnitude, due to increasing errors in the measured colors of fainter and more distance stars in a given survey. Since the FTO stars were selected based on color, the sample is significantly contaminated by stars of different types as the color errors increase [3].

Newby et al. (2011) used eleven globular clusters in the Northern Galactic Cap from SDSS DR7 in their analysis. They spanned ages from 9.5 to 13.5 Gyr and metallicities from [Fe/H]$= -1.17$ to [Fe/H]$= -2.30$. The similarity in the absolute magnitudes of the FTO stars was surprising, but is apparently due to the Milky Way Age-Metallicity Relationship (AMR) [13, 14, 15] recently discussed by DeAngeli (2005), Marín-Franch (2009), and Dotter (2011). Younger clusters would normally have a brighter turnoff than older clusters, as fewer high-mass stars would have burned out and left the main sequence. Metal-rich clusters usually have fainter turnoffs. Since metal-rich clusters are generally younger than metal-poor clusters, the effects cancel so that the turnoff distribution is largely the same for globular clusters in the Milky Way. Newby et al. (2011) showed that the similarity in turnoff distributions for old populations in the Galactic halo simplifies measurements for distances but complicates estimates for age. Both age and metallicity affect the turnoff magnitude and color of a cluster.

In this paper, we apply the techniques from Newby et al. (2011) to see if the conclusions hold for two additional globular clusters in the Southern Galactic Cap that became available in a later SDSS data release [16]. One cluster has an age and metallicity within the range for clusters chosen by Newby et al. (2011), while the second cluster is younger and more metal-rich than the previous clusters studied. Both clusters studied are more distant than any of the clusters studied by Newby et al. (2011), so our study tests the predictions for higher color errors than previously studied. We present color-magnitude diagrams and isochrones for each cluster. We also show histograms of the magnitude distribution of color-selected FTO stars, which are compared with the predictions of Newby et al. (2011). The mean value of a histogram of the magnitudes of stars for each cluster also marks the bluest point on the cluster's isochrone. We conclude that the mean magnitude of FTO stars in these globular clusters in the Milky Way are consistent with the results of Newby et al. (2011), though these clusters are more distant and one is at a higher metallicity than previously

studied.

2 Globular Cluster Data Selection

In the Catalog of Parameters for Milky Way Globular Clusters [17] there are three clusters in the Milky Way halo that are in the Southern Galactic Cap portion of the SDSS footprint. One of the three clusters, NGC 7089, was included in the studies by Newby et al. (2011). The other two are Palomar 13 and Whiting 1.

Palomar 13 was studied using the Keck telescope and High Resolution Echelle Spectrometer (HIRES) by Côté et al.(2002) [18] to estimate a distance of 24.3 kpc, equivalent to the distance given by [17]. Bradford et al. (2011) [19] used the Keck/DEep Imaging Multi-Object Spectrograph (DEIMOS) to determine a spectroscopic metallicity of [Fe/H]=-1.6 and an age of 12 Gigayear (Gyr) for Palomar 13. Whiting 1 was originally reported by Whiting et al. (2001)[20] and was subsequently studied by Carraro et al. (2007) [21] using BVI photometry and color-magnitude diagrams to obtain an estimated age of $6.5^{+1.0}_{-0.5}$ Gyr, a metallicity of Z=0.004 ([Fe/H]=-0.65) and a distance of 29.6 kpc, which is closer than the estimate from [17].

To build our data set for each globular cluster, we used the coordinates from [17] to center the globular cluster in the SkyServer Navigate Tool. We magnified the cluster within the frame so that the cluster was visible and visually distinct from the background. The Right Ascension and Declination (α, δ) values were read from the corners of the image, 0.5 degrees from the center of the clusters, and the square area of stars was selected from the SDSS database. The selection limits for Palomar 13 were $347.0^o < \alpha < 364.45^\circ$ and $12.4^\circ < \delta < 13.0^\circ$. The selection limits for Whiting 1 were $30.05^\circ < \alpha < 31.05^\circ$ and $-3.55^\circ < \delta < -3.0^\circ$. We queried the SDSS database over the area chosen for each cluster, selecting objects classified as "star" with colors in the range $-0.3 < (g-r)_0 < 0.6$ to include a wide range of stars, including FTO stars, and $(u-g)_0 > 0.4$ to eliminate quasars [5].

The selected stars are shown in Figure 1. The selected stars that are more than 0.037 degrees from each cluster were included in "background" samples. We removed the stars that were located in an annulus with a width of 0.02 degrees at the boundary of the cluster and background stars to remove contamination from background stars. These stars are not shown in the figure.

3 Isochrone Fits

In Figures 2 and 3 we show color-magnitude diagrams of the stars in each globular cluster, and of the stars in a region around each globular cluster, respectively. The background stars are at different distances, have different ages, and should not group together on a color-magnitude diagram in the same way that globular

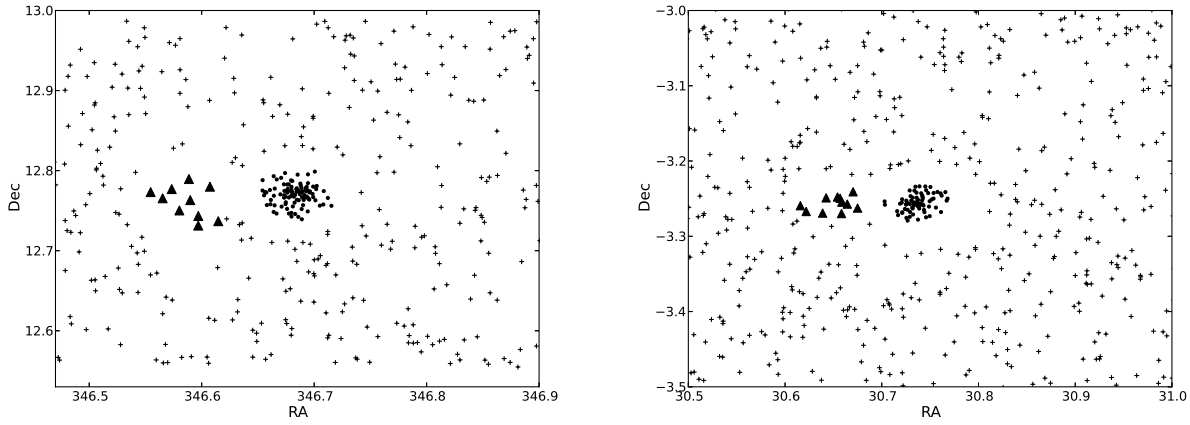

Figure 1: Right Ascension and Declination positions of stars in Palomar 13 on the left and Whiting 1 on the right. In each panel, cluster stars are marked with filled circles, and background stars are marked with plus signs. Stars within an annulus of width 0.02 degrees been discarded at the boundary between the cluster and backgrounds stars to prevent contamination in the cluster and background samples. A sample of the background the same angular size as the cluster is marked with solid triangles.

cluster stars do. There is a lack of stars with a magnitude fainter than 22 in the figures, because the fainter stars in globular clustersare obscured by brighter ones [5]. Outside of the globular clusters, the SDSS is efficient at detecting sources to 23rd magnitude in g. The FTO stars attributed to the cluster have a range of about 2 magnitudes. In both panels of Figure 2 and the right panel of Figure 3, most of the stars are bluer than $(g-r)_0$=0.4. In the left panel of Figure 3, there is a higher density of stars redder than $(g-r)_0 = 0.4$

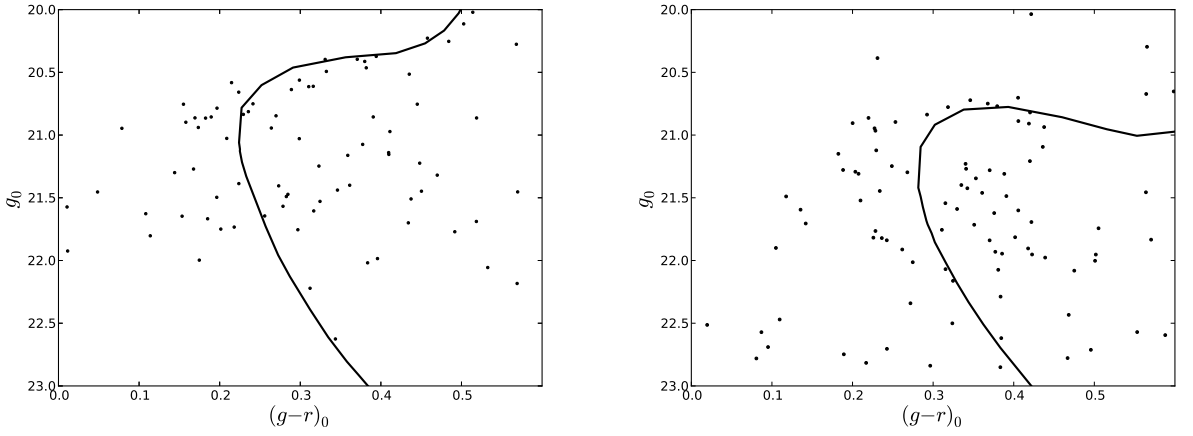

Figure 2: Color-magnitude plots for Palomar 13 (left) and Whiting 1 (right) are shown with isochrones overlaid. We used an age of 12 Gyrs and a metallicity of Z=0.00039 for Palomar 13 [19]. We used an estimated age of 6.5 Gyrs and a metallicity Z=0.004 for Whiting 1 [21]. The third parameter, distance, was 24.3 kpc [18] for Palomar 13 and 30.1 kpc [17] for Whiting 1. The data has a large scatter in color, but the isochrones fit the data. Because faint stars are overpowered by brighter stars in crowded parts of the sky like globular clusters, there are few stars fainter than the 22^{nd} magnitude.

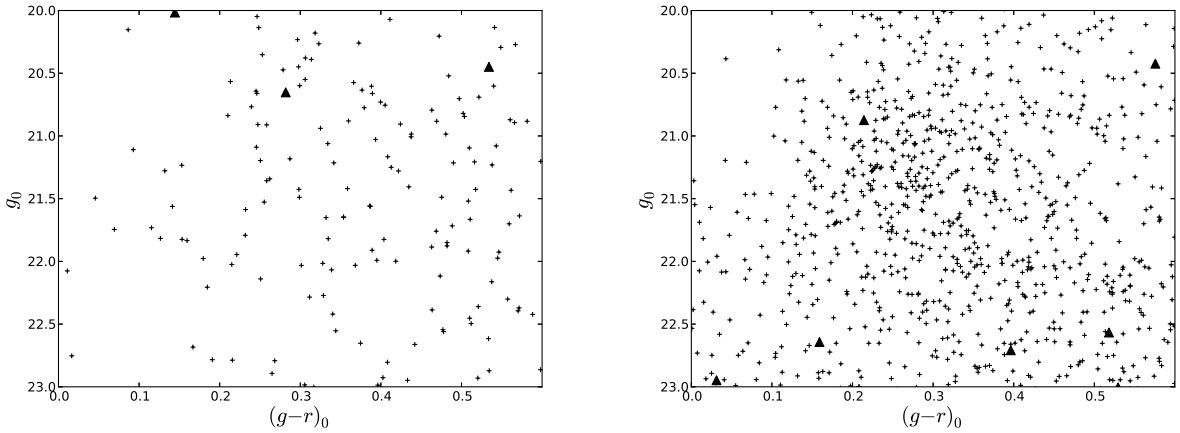

Figure 3: A color-magnitude diagram for background stars near Palomar 13 on the left and near Whiting 1 on the right. The solid triangles show the positions of stars from a sample of the background with the same area as the globular cluster. Not all of the triangles depicted in Figure 4 are visible here because the magnitudes are not in the range shown. The scatter of stars is indicative of a good choice in background. The background of Whiting 1 shows the main sequence of the Sagittarius tidal stream.

Unlike closer globular clusters, it is difficult to pinpoint the turnoff of these clusters because they are close to the magnitude limits of the SDSS photometry and the errors in color are large. Also, much of the main sequence below the turnoff is not visible. Instead of fitting an isochrone to the data, we used the accepted values from other sources for the age and metallicity for each cluster. Following Newby et al. (2011), we used the linear color correction from [3] to calibrate the Padova isochrones [22, 23] to An et al. (2009) [24] results.

For Palomar 13, we used a metallicity of [Fe/H]= -1.7 and Z=0.00039 and an age of 12 Gyrs [19]. For Whiting 1, we used a metallicity [Fe/H]=-0.65 and Z=0.004, and an estimated age of the cluster of 6.5 Gyr from photometry measurements [21]. In the HR diagrams for both clusters, there is a concentration of stars at about the right color and magnitude for the cluster turnoff. Due to the large distances of these clusters, the observed color spread of the turnoff is large and the fraction of cluster stars observed is reduced. The color-magnitude diagram for stars in Palomar 13 has few stars with a magnitude fainter than 22 due to the crowding and cluster detection efficiency at faint magnitudes [5]. A decrease in the number of stars fainter than the 22nd magnitude is also evident in the HR diagram for Whiting 1.

The left panel of Figure 2 shows a color-magnitude diagram of Palomar 13 cluster stars where the stars group together and follow the shape of the isochrone. The left panel of Figure 3 shows a color-magnitude diagram of the background stars from Figure 1, showing an even and apparently random distribution of stars. They do not clump around the isochrone. A small area of the background in Figure 1 was chosen to have the same area in the sky as the cluster and was plotted as solid triangles, to show the expected density

of stars that are not part of a cluster. Only three of ten stars are in the portion of the HR diagram shown and they do not follow the same pattern as the color-magnitude diagram for the cluster in Figure 2.

The right panel of Figure 2 shows a color-magnitude diagram of Whiting 1 cluster stars. The isochrone shows that the concentration of stars is near the expected turnoff magnitude. In the right panel of Figure 3, the sample of background chosen to have the same angular size as the clusters are denoted by solid triangles. The background is not part of the cluster, so it is surprising that many of the background stars seem to follow the isochrone.

The magnitude versus color distribution of the background stars selected around Whiting 1 looks similar to the distribution of Whiting 1 itself. It is unusual to find that the stars outside a globular cluster have the same distribution in an HR diagram as the cluster itself. In this case, we believe this is due to the globular cluster's association with the Sagittarius dwarf tidal stream. Law and Majewski (2010)[25] found that Whiting 1 was likely to be part of the trailing tail of the Sagittarius dwarf stream based on angular position, heliocentric distance, and radial velocity. These stars, and possibly the Whiting 1 globular cluster, were ripped away from the Sagittarius dwarf spheroidal galaxy by the tidal forces in the Milky Way.

Though Palomar 13 was originally a candidate for association with the Sagittarius stream, the proper motions from Siegel (2001)[26] led them to conclude that it is not likely that Palomar 13 was part of the Sagittarius stream. We agree with these results, as stars from the Sagittarius dwarf tidal stream do not appear in the background of Palomar 13.

4 Measured versus Expected F-Turnoff Absolute Magnitude Distribution

The globular clusters studied in Newby et al. (2011) had similar μ and σ_ℓ values (where μ is the peak turnoff star absolute magnitude and σ_ℓ is the width of the left side of the Gaussian) regardless of distance, age, or metallicity. This implies that the halo cluster populations are intrinsically similar. There were differences in the measured values of σ_r due only to observational biases in SDSS photometry at faint magnitudes. Equation 12 [3] provides a fourth order polynomial fit to σ_r as a function of distance due to color errors

$$1.741633 + 0.457079d - 0.0250001d^2 + 5.720776 \times 10^{-4}d^3 - 4.7 \times 10^{-6}d^4. \quad (1)$$

This formula is only valid for 10¡ d¡ 45 kpc. Errors in colors at large distances reduced the number of true FTO stars detected on the faint side of the histogram, but increased the number of intrinsically redder and fainter stars. The intrinsic value of 0.76 ± 0.04 presented for σ_r is an error-weighted average of the four

closest clusters, which are consistent with each other and have little contamination from red main-sequence stars.

The μ (mean absolute magnitude) determined by Newby et al. (2011) was 4.18 ± 0.008 and σ_ℓ (bright-side σ) was 0.36 ± 0.006 [3] based on the parameter fits to the 11 clusters studied. Figure 16 of Newby et al. (2011) was used to determine the expected faint side width, σ_r, for the two clusters studied here. The faint-side width is affected by the size of the cluster and the distance to the cluster. As the distance to the cluster increases, photometric color errors increase and red main sequence stars leak into the color selection range. At a distance of about 25 kpc away, the contamination from red stars stops increasing as these faint stars begin to fall below the SDSS apparent magnitude detection threshold [3]. The central regions of clusters are often excluded from the SDSS database, as the photometric pipeline was not well-suited for resolving crowded stars. Our two clusters are at such a large distance that only the bright stars are detected, as the fainter stars are washed out or beyond the magnitude limit of the survey.

We apply the same techniques as Newby et al. (2011) to determine whether or not Palomar 13 and Whiting 1 agree with the previously studied clusters. To determine the turnoff using magnitude alone, we made a histogram for each of the globular clusters with bin widths of 0.2 magnitudes. We chose a range of $0 < M_g < 8$, but did not fit to stars with a calculated absolute magnitude brighter than 2 to reduce the chance of binning stars that are not from the cluster.

For each cluster, we used all of the photometric data in Figure 1 to make a histogram of the cluster stars and a separate histogram for the background. We scaled the background histogram to the area of the cluster and subtracted it from the cluster histogram. We then fit a "double-sided" Gaussian distribution to each cluster where the standard deviation is different on each side of the mean. The form of the fit function [3] is

$$G(M_g : \mu, \sigma_\ell, \sigma_r, A) = A \cdot exp\left[\frac{-(M_g - \mu)^2}{2\sigma_i^2}\right] \tag{2}$$

where $\sigma_i = \sigma_\ell$ if $M_g \leq \mu$ and $\sigma_i = \sigma_r$ if $M_g \geq \mu$. When normalized,

$$A = (2\pi[\frac{\sigma_\ell + \sigma_r}{2}]^{-1/2}). \tag{3}$$

The parameters $\mu, \sigma_\ell, \sigma_r$, and A are the magnitude at the peak of the population, the standard deviation of the left side, the standard deviation of the right side, and the amplitude, respectively. The amplitude, A, is dependent on the number of stars included in the cluster studies and will vary for each cluster. Since the true Poisson counting errors are given by $\sqrt{N+1}+1$, the minimimum error on a bin height is 2 counts so we do not expect bins with less than 4 counts to significantly affect the fit distribution. A two-stage χ^2

minimization process avoided local minima and accurately determined the values of the parameters. We used a Markov Chain Monte Carlo technique to inspect equilibrium points and then input those points into a gradient descent algorithm to locate the global minimum.

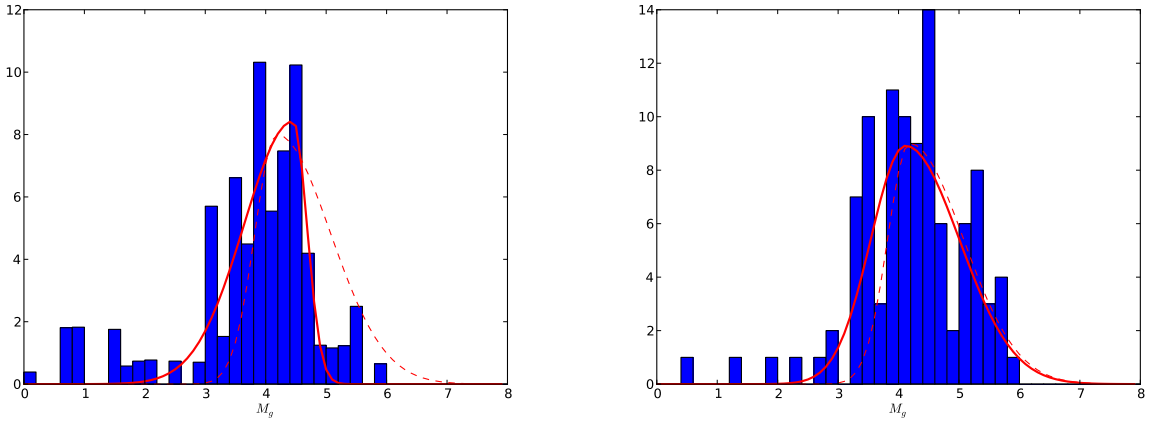

Figure 4: Histogram of absolute magnitudes of Palomar 13 on the left and Whiting 1 on the right. In both plots, the dashed line shows the double-sided Gaussian expected for each cluster with the values obtained from Newby et al. (2011). The solid line in each plot fits a double-sided Gaussian distribution to the histogram.

We present the absolute magnitude and best-fit Gaussian for Palomar 13 in the left panel of Figure 4. The dashed line is the double-sided Gaussian distribution fit anticipated by the values determined by Newby et al. (2011)[3], and the solid line is the double-sided Gaussian fit to Palomar 13 data. The μ value, or the turn-off absolute magnitude, is 4.46 ± 0.26 for the parameter fit. This corresponds to the leftmost and bluest point of the isochrone in Figure 3 at a color $(g-r)_0 = 0.22$. This shows that using the histogram of magnitudes for FTO stars in the cluster yields the same turnoff color and magnitude as the Padova isochrones, given the published age and metallicity. The value predicted from Newby et al. (2011) is $M_g = 4.18 \pm 0.008$. The mean absolute magnitude for this cluster deviates from the value from Newby et al. (2011) by slightly more than 1σ, where σ is the error in M_g.

The measured σ_ℓ and σ_r values for Palomar 13 are 0.81 ± 0.25 and 0.226 ± 0.23, respectively. The σ_ℓ value for Palomar 13 is much higher than the expected value of 0.36 ± 0.006 [3], but still within 2σ. Though the stars with a magnitude between 0 and 2 were not included in the data analysis to prevent contamination from foreground stars, there is a larger magnitude spread of stars brighter than the mean magnitude than fainter. The expected value of σ_r was 0.89 [3] including the bias against observing faint stars in globular clusters in the SDSS. The value we obtained is almost 3 standard deviations lower than the prediction and there are not very many stars with absolute magnitudes fainter than 5. [5]. The amplitude fit, A, for the double-Gaussian distribution for Palomar 13 is 8.44 ± 2.22. The amplitude is different for every cluster; the

more cluster stars observed, the larger the amplitude of the Gaussian fit.

The absolute magnitude histogram and the best-fit Gaussian for Whiting 1 are shown in the right panel of Figure 4. The dashed line is the double-sided Gaussian distribution fit anticipated by the values determined by Newby et al. (2011) [3]. The measured and expected Gaussians correspond well on the right side of double-sided Gaussian distributions, but have a larger standard deviation on the left side. The measured mean turnoff absolute magnitude, μ, is 4.11 ± 0.3. The μ value anticipated by Newby et al. (2011) of 4.18 ± 0.008 is well within the errors. The σ_ℓ parameter for the fit of the data is 0.57 ± 0.25. The expected value of 0.36 ± 0.006 is consistent with the fit values within the errors. The fit value for σ_r is 0.86 ± 0.27, compared to the expected value of 0.76 at this distance. Again, this fit value is consistent within errors with the expected value. The amplitude fit, A, for the double-Gaussian distribution for Whiting 1 is 8.91 ± 1.86.

The expected and observed magnitude distributions for Whiting 1 agree within 1σ error bars. The mean magnitude and the bright side sigma for Palomar 13 agree with the expected values within 2σ. The faint side error is nearly 3σ lower than the expected and there are very few stars with a magnitude fainter than 5. There are fewer faint stars in Palomar 13 than expected. Whiting 1 is the most distant and most metal-rich cluster, so we were surprised that Palomar 13 was the cluster that differs from Newby et al. (2011) results. We suspect the disagreement is the result of poorer seeing in the Palomar 13 image, which affects teh width of the point-spread-function. All of the data for Palomar 13 is contained in one run, and the width of the point-spread function in the r filter is over 2", which is outside of the usual image quality limit in SDSS. For comparison, the width of the point-spread function in the r filter for stars in Whiting 1 ranges from 1.33" to 1.58". The poor seeing will increase the chance that fainter stars will be obscured by brighter stars in a globular cluster, and likely leads to the apparent lack of fainter turnoff stars.

5 Age-Metallicity Relationship

Newby et al. (2011) showed that their cluster sample was consistent with the assumed Age-Metallicity Relationship (AMR) for the Galaxy, and that this AMR is the underlying reason for the similar intrinsic turnoff properties of old halo clusters. Since supernovae will enrich star-forming clouds with metals as the Universe ages, the formation time of a cluster should correlate with its metallicity, such that metallicity decreases as age increases. Recent observational evidence [13, 14, 15] suggests that this relationship is more complicated for globular clusters in the Milky Way, with several clusters having very old ages ($\sim$13 Gyr) but a wide range of metallicities. These constant-age clusters are thought to be coeval with the Milky Way's initial formation event, which is thought to have consisted of rapid star formation and metal enrichment in a short span of time [15]. Figure 17 of Newby et al. (2011) illustrated that their studied clusters were consistent

with the decreasing-metallicity-with-age-trend (the AMR), and we reproduce that plot, with Whiting 1 and Palomar 13 added, as Figure 5.

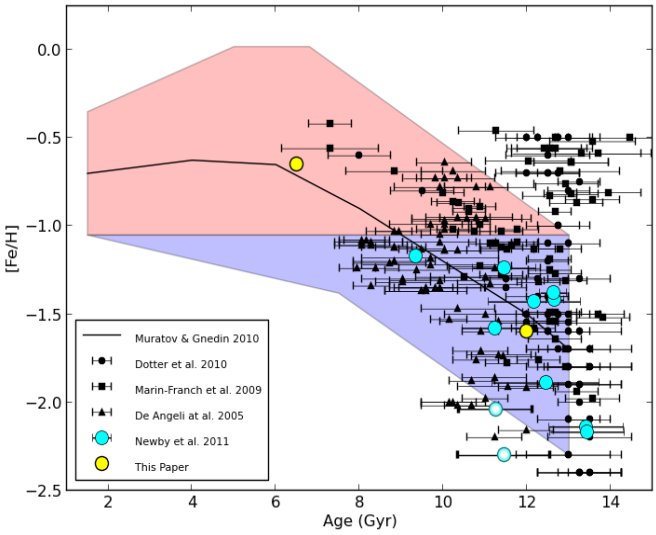

Figure 5: Here Figure 17 from Newby et al. (2011) is reproduced, with permission, with the addition of our new clusters. The plot of age versus metallicity for Milky Way globular clusters includes different sources, where clusters studied by Newby et al. (2011) are denoted by blue circles and the two clusters from this study indicated by yellow circles. The mean value of the theoretical AMR from Muratov and Gnedin (2010) is indicated by the solid line. The shaded areas show the spread of metallcities for a given age as shown in Muratov & Gnedin (2010), where blue and red correspond to old and young globular cluster populations, respectively.

Clusters that lie along the halo cluster AMR, a theoretical model for which was recently presented in Muratov & Gnedin (2010), have remarkably similar turnoff star properties. As a cluster ages, the turnoff color becomes fainter and redder as brighter, bluer stars evolve off of the main sequence. Metal-poor stars, however, are bluer and brighter than analogous metal-rich stars. Newby et al. (2011) remarked that along the average halo cluster AMR, these competing properties almost entirely canceled each other out, resulting in intrinsically similar turnoff colors and absolute magnitudes for old halo globular clusters. We see from Figure 5 that our clusters are surprisingly consistent with the halo cluster AMR.

The plot of age versus [Fe/H] metallicity in Figure 5 includes the mean metallicity at a range of ages [27] plotted as a solid line, and we find that Palomar 13 is close to the AMR with an age of 12 Gyr and [Fe/H]=1.7 in the metal-poor region [19] and Whiting 1, with [Fe/H]=-0.65 and an age of 6.5 Gyr [21], is also close to the solid line, but in the metal-rich region.

We plot the Padova isochrones of clusters in this study in Figure 6 against theoretical isochrones for similar age and metallicity values along the average cluster AMR. The filled circles correspond to the isochrone for

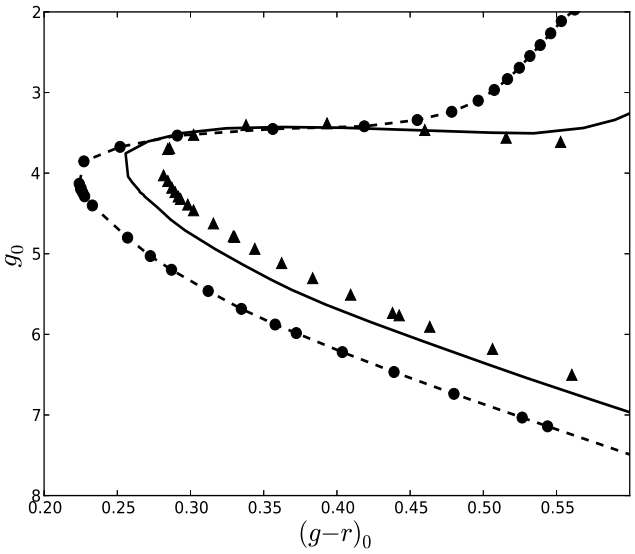

Figure 6: We plot the Padova isochrones from Figure 2 for Palomar 13 and Whiting 1 in addition to two theoretical isochrones chosen from Figure 18 of Newby et al. (2011) to compare the turnoff locations of combinations of age and metallicity. The black triangles correspond to the isochrone for Whiting 1 with an age of 6.5 Gyrs and a metallicity [Fe/H] of -0.65. The dashed line overlapped by filled circles represents a cluster 12 Gyrs old with a metallicity [Fe/H] of -1.7, which are the estimates for Palomar 13. The solid line represents a cluster 8 Gyrs old with a metallicity of -0.9. From left to right, the age decreases and metallicity increases.

Palomar 13, which lies almost exactly on the average AMR line and so coincides exactly with the dashed black isochrone, which is a hypothetical cluster on the AMR with [Fe/H]=-1.7 and an age of 12 Gyr. The triangles correspond to the isochrone created for Whiting 1. The central solid line is an isochrone for a cluster 8 Gyr and [Fe/H]=-0.9, which is the oldest and most metal-poor cluster analyzed by Newby et al. (2011). Though the ages range from 12 Gyrs to 6.5 Gyrs, the color and magnitude of the FTO stars are similar, hardly differing in turnoff magnitude, and the color differs by less than 0.1 in $(g-r)_0$. As the turnoff colors approach the edge of the color selection box for FTO stars, Whiting 1 may represent the very youngest of clusters for which the Newby et al. (2011) method can be applied.

6 Conclusions

In this paper, we analyze two globular clusters in the Milky Way halo using the techniques of Newby et al. (2011). We create a histogram of the absolute magnitudes for each cluster. We fit a double-sided Gaussian to each histogram and compared it to the results for parameters reported by Newby et al. (2011).

For Palomar 13, the absolute magnitude histogram fit parameters μ, σ_ℓ, and σ_r are 4.46±0.26, 0.81±0.025, and 0.2226 ± 0.23, respectively. Similarly, the magnitude histogram fit parameters for Whiting 1 are $\mu =$

4.11 ± 0.3, $\sigma_\ell = 0.57 \pm 0.25$, and $\sigma_r = 0.86 \pm 0.27$. The Whiting 1 parameters agree with the expectations from Newby et al. (2011). The Palomar 13 results are marginally different, at the two and three sigma level.

We believe the smaller number of faint stars oserved in Palomar 13 is due to larger seeing in the SDSS image for that cluster, and not due to an intrinsic difference in the absolute magnitude distribution of turnoff stars in that cluster.

The similarity of the Whiting 1 results allows us to extend the region of applicability of the Newby et al. (2011) results to halo globular clusters as young as 7 Gyr, metallicities as high as [Fe/H]=-0.7, and to distances as high as 30 kpc.

We support the conclusion of [25] that Palomar 13 is not a member of the Sagittarius dwarf tidal stream, while Whiting 1 is within the Sagittarius dwarf tidal stream.

7 Acknowledgements

We thank the anonymous reviewer for insightful feedback to improve the clarity of the paper.

This research is based upon work supported by the National Science Foundation under Grant No. AST 10-09670.

Funding for SDSS-III has been provided by the Alfred P. Sloan Foundation, the Participating Institutions, the National Science Foundation, and the U.S. Department of Energy Office of Science. The SDSS-III web site is http://www.sdss3.org/.

SDSS-III is managed by the Astrophysical Research Consortium for the Participating Institutions of the SDSS-III Collaboration including the University of Arizona, the Brazilian Participation Group, Brookhaven National Laboratory, University of Cambridge, Carnegie Mellon University, University of Florida, the French Participation Group, the German Participation Group, Harvard University, the Instituto de Astrofisica de Canarias, the Michigan State/Notre Dame/JINA Participation Group, Johns Hopkins University, Lawrence Berkeley National Laboratory, Max Planck Institute for Astrophysics, Max Planck Institute for Extraterrestrial Physics, New Mexico State University, New York University, Ohio State University, Pennsylvania State University, University of Portsmouth, Princeton University, the Spanish Participation Group, University of Tokyo, University of Utah, Vanderbilt University, University of Virginia, University of Washington, and Yale University.

References

[1] York, D. G., Adelman, J., Anderson, J. E., Jr., et al. 2000, AJ, 120, 1579

[2] Schlegel, D. J., Finkbeiner, D. P., & Davis, M. 1998, ApJ, 500, 525

[3] Newby, M., Newberg, H. J., Simones, J., Cole, N., & Monaco, M. 2011, ApJ, 743, 187

[4] Piotto, G., Milone, A. P., Anderson, J., et al. 2012, arXiv:1208.1873

[5] Newberg, H. J., Yanny, B., Rockosi, C., et al. 2002, ApJ, 569, 245

[6] Yanny, B., Newberg, H. J., Kent, S., et al. 2000, ApJ, 540, 825

[7] Newberg, H. J., & Yanny, B. 2006, Journal of Physics Conference Series, 47, 195

[8] Yanny, B., Newberg, H. J., Grebel, E. K., et al. 2003, ApJ, 588, 824

[9] Yanny, B., Newberg, H. J., Johnson, J. A., et al. 2009, ApJ, 700, 1282

[10] Newberg, H. J., Willett, B. A., Yanny, B., & Xu, Y. 2010, ApJ, 711, 32

[11] Willett, B. A., Newberg, H. J., Zhang, H., Yanny, B., & Beers, T. C. 2009, ApJ, 697, 207

[12] Cole, N., Newberg, H. J., Magdon-Ismail, M., et al. 2008, ApJ, 683, 750

[13] De Angeli, F., Piotto, G., Cassisi, S., et al. 2005, AJ, 130, 116

[14] Marín-Franch, A., Aparicio, A., Piotto, G., et al. 2009, ApJ, 694, 1498

[15] Dotter, A., Sarajedini, A., & Anderson, J. 2011, ApJ, 738, 74

[16] Aihara, H., Allende Prieto, C., An, D., et al. 2011, ApJS, 193, 29

[17] Harris, W. E. 1996, AJ, 112, 1487

[18] Côté, P., Djorgovski, S. G., Meylan, G., Castro, S., & McCarthy, J. K. 2002, ApJ, 574, 783

[19] Bradford, J. D., Geha, M., Muñoz, R. R., et al. 2011, ApJ, 743, 167

[20] Whiting, A. B., Hau, G. K. T., & Irwin, M. 2002, ApJS, 141, 123

[21] Carraro, G., Zinn, R., & Moni Bidin, C. 2007, A&A, 466, 181

[22] Marigo, P., Girardi, L., Bressan, A., et al. 2008, A&A, 482, 883

[23] Girardi, L., Bressan, A., Bertelli, G., & Chiosi, C. 2000, A&AS, 141, 371

[24] An, D., Pinsonneault, M. H., Masseron, T., et al. 2009, ApJ, 700, 523

[25] Law, D. R., & Majewski, S. R. 2010, ApJ, 718, 1128

[26] Siegel, M. H., Majewski, S. R., Cudworth, K. M., & Takamiya, M. 2001, AJ, 121, 935

[27] Muratov, A. L., & Gnedin, O. Y. 2010, ApJ, 718, 1266